Experimental study on the mechanical properties and structural performance of the rapid hardening concrete

Mohamed Hussein Elfakhrany[1*] , Amal Zamrawi[1], Wael Ibrahim[1] and Alaa Sherif[1]

*Correspondence:
engmohamedhussein04@gmail.com

[1] Civil Department, Faculty of Engineering, Helwan University, Cairo, Egypt

Abstract

Rapid-hardening concrete (RHC) is becoming more popular as a cast-in-place jointing material in precast concrete bridges and buildings due to its high tensile strength and crack resistance. RHC's technical properties are highly regarded due to the working conditions of mega projects. The study assessed the impact of modern modifiers on concrete in order to select a composition of rapid-hardening concrete (RHC) with superior mechanical properties. Following an analysis of previous studies by other authors, microsilica and a polycarboxylate ether-based chemical additive was chosen as basic modifiers in the manufacture of RHC. In addition, four reinforced rapid-hardening concrete beams were tested for operational reliability and durability after 3 days of casting. The structural performance of RHC beams was evaluated in comparison to normal concrete beam specimens, and it was determined that crack distribution, load deflection, reinforcement strains, ductility, and toughness were all important factors in the evaluation. RHC beams exhibit higher ductility, toughness, ultimate loads, and deformability than NC beams. The tensile strength analysis revealed a positive impact of RHC, but the shrinkage crack related to heat hydration was crucial.

Keywords: Self-compacting, RHC, Normal strength, Workability, Temperature, Mechanical behaviour

Introduction

Modern construction requires a fast rate of execution, especially in monolithic construction [1]. The main economic indicator of monolithic house-building is the shortening of the time required for constructing one floor to 3 days [2, 3]. Smart city design eliminates guesswork in design, resulting in sustainable designs with minimal time/funds [4]. The rapid attainment of design strength for monolithic structures necessitates this technical requirement due to commercial necessity. To improve the productivity of construction activities, it is crucial to increase the turnover of molds and formwork, use equipment that is highly effective, and maximize efficiency [5]. Rapid hardening concrete (RHC) is commonly known as concrete with accelerated strength gain and can be used to achieve a fast construction pace [6]. RHC is a concrete that can reach acceptable compressive and flexural strength within a few hours [7]. It is possible for the compressive strength

to reach structural concrete quality during the first 24 h of site pouring when it exceeds 21 MPa [8]. Some research on concrete technology was conducted to produce rapid hardening concrete with several approaches. Such as using several types of cement (type I cement, type III cement, rapid set cement) and a high cement content (400–800 kg/m^3) [9]. Maintain a low water to cementitious ratio (0.2 to 0.4) by using a variety of admixtures, including calcium chloride and polycarboxylate ether. Consequently, compressive strength values could reach 39 to 66 MPa after 24 h [10]. The use of a high amount of cement and a low w/c ratio can lead to thermal strains that can lead to cracking and loss of durability, which is a major drawback of manufacturing RHC [11–13].

The search for concrete that hardens quickly and has high early strength to repair bridge decks without causing traffic disruption has become a top priority. This reason led to the creation of a new rapid hardening concrete that uses polycarboxylate ether instead of calcium chloride. The demand for better behavior and lower costs has resulted in more research being conducted on upgrading or exploiting structural mechanical performance by introducing innovative materials, structures, and techniques [14–23]. For the composition of rapid hardening concrete, in this research, the presence of microsilica reactive admixture and nanoparticles is used to improve defective and porous structures within the concrete [24]. Thus, the concrete material's durability improves while its permeability to chloride ions reduces. Moreover, fine quartz sand was utilized to enhance the compactness and uniformity of the aggregate by not mixing coarse aggregate [25]. The use of cement type III instead of cement type I resulted in fewer thermal results from the internal chemical reaction that occurs during the cement hydration process [26]. Polycarboxylate ether and other recent chemical additives ensure the fluidity of the fresh concrete and solve the problem of densely formed elements caused by the short setting time of RHC.

However, the mechanical properties of rapid hardening are still unclear, which hinders the application of this innovative type of concrete [27]. The mechanical properties of concrete are the main performance indicators, which determine the load-bearing capacity of structures such as tunnels and bridges. Despite this, it is regarded as a significant foundation for structural design and construction. Rui Yu et al. [28] conducted an experimental study on rapid hardening concrete. The experimental results indicated that the strength of 3 h developed fastest at 55 MPa when the gypsum substitution rate was 15%, while the later strength could be continuously increased to 81 MPa after 7 days. The Strategic Highway Research Program [8] provided information on materials and concrete aggregate sources in four regions of America to achieve compressive strength greater than 35 MPa in 24 h. AL-Manaseer et al. [29–31] Complete experimental data was obtained using specific cement types that contain proprietary compounds to achieve early-strength concrete mixes. Dharm Bhatt et al. [32] perform RHC mixes with six types of cement. The compressive strength reached 13.7 Mpa within 3 h, and the modulus of rupture was 2.4 MPa, but it was workable for about 20 min. The Federal Highway Administration [33] experimented with various mix patterns to produce concrete with excellent early strength, enabling traffic to reopen within 4–6 h. Najm et al. [34] investigate the influence of cement type, content, water-cement ratio, admixtures, and temperature on the properties of RHC. The value of this comprehensive study lies in its valuable insights that can be used to optimize mix design and ensure desired strength

and workability. Yelbek Utepov [35] tackles the challenge of frost resistance in RHC. By using micro silica and CaCl2 modifiers, the researchers achieved a good performance in freeze–thaw cycles, expanding the potential applications of RHC in cold climates. Cangiano [36] performed RHC produced with commonly available raw materials and did not contain any silica fume or other pozzolanic materials or accelerating admixtures. The concrete mix had a water-to-cement ratio of 0.45 and a compressive strength of 40 MPa at 1 day and 60 MPa at 28 days. Gabriel Cook [37] studied the flexural performance of reinforced BCSA concrete beams. Wael et al. [38] examined the flexural behavior of reinforced rapid-hardening concrete beams to calculate peak load, displacement, and flexural strength. Jacek [39] tested high-performance, high early strength concretes, which were tested for compressive strength without the use of heat. It has been established that utilizing Portland cement CEM I 52.5 R instead of CEM II/A-S 52.5N reaches a compressive strength of 36 MPa after 16 h. Despite the above-mentioned investigations of rapid hardening concrete, few studies have focused on the mechanical properties of rapid hardening concrete.

The results of this research have a significant implication for the production of construction work. The rapid hardening concrete obtained in this study will be particularly useful in construction projects in which a quick turnaround time is required, while the structural performance of concrete beams is an important element in structures.

The objective of this research

This study aims to evaluate the mechanical and structural performance of RHC, which contains microsilica and polycarboxylate ether and is intended for use in concrete elements. The influence of temperature is more significant in the design of mixes. Samples were tested for workability, compressive strength, and tensile strength. The best mixes were used to assess the flexural performance of four reinforced RHC beams, which were then compared to normal-strength reinforced concrete beams.

Selection of materials

Cement and micro silica

As per ECP203-2020 [40], there are various types of cement that can be utilized for the production of rapid hardening concrete. But in this experimental study the rapid hardening concrete utilized by Cem I and Cem III. Laboratory tests were carried out to obtain the physical and chemical properties of the cement and microsilica as illustrated in Table 1.
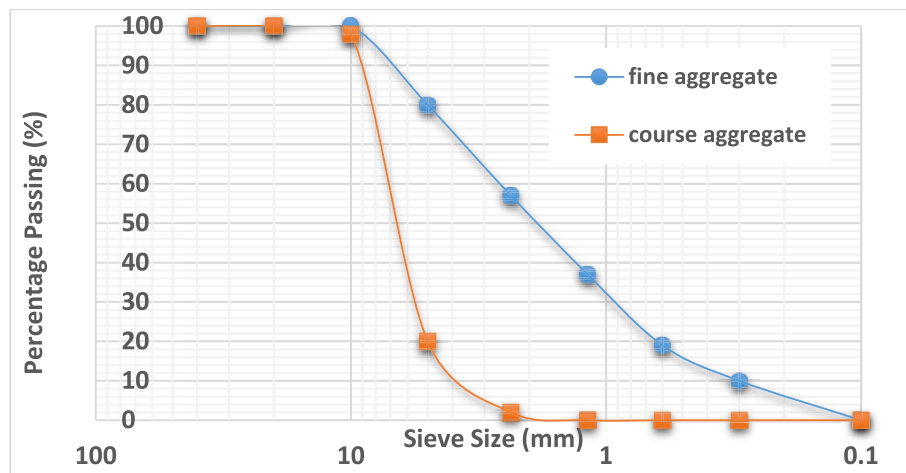
Coarse aggregate

As per ECP203-2020 [40], Crushed dolomite was utilized as the coarse aggregate, with a nominal maximum size of 10 mm with a fineness modulus of 4.8 and a specific gravity of 3.15. The coarse aggregate used was free of impurities and did not contain any organic compounds or honeycomb.

Fine aggregate

As per ECP203-2020 [40], the fine aggregate used in this work is natural sand composed of siliceous materials with a fineness modulus of 2.9. The fine aggregates were clean, free

Table 1 Chemical and physical properties of cement and microsilica

Component/property			Cem I	Cem III	Micro silica
Chemical composition (%)	SiO_2		21.5	30	96.2
	AL_2O_3		6.0	6.2	0.64
	Fe_2O_3		3	1.7	0.3
	CaO		61.2	50.3	0.61
	MgO		2.2	5.0	0.03
	K_2O		0.95	0.7	0.36
	SO_3		3.1	2.4	0.05
	Na_2O		–	–	0.2
	Loss on ignition		2.4	2.5	1.32
	Insoluble residue		0.9	0.95	–––-
Physical and mechanical properties	Specific gravity		3.15	3.0	2.15
	Specific surface area (cm^2/g)		3540	3000	264,500
	Setting time (min)	Initial	120	160	–––-
		Final	180	195	–––-
	Soundness (mm)		1	1	–––-
	Compressive strength (N/mm^2)	3 days	40	30	–––-
		28 days	60	50	–––-

Fig. 1 Grading curves for fine aggregate and coarse aggregate

of impurities, and with no organic compounds. The grading curve of fine and coarse aggregate is shown in Fig. 1.

Mixing water

As per ECP203-2020 [40], clean fresh drinking water was used free from impurities, oils, acids, and alkalis for mixing and curing all concrete specimens in this work.

Superplasticizers

Superplasticizers meet the requirements of ASTM C-494 [41] types G and F. This type of admixture has a long-chain molecular structure that contributes to the production of

high-fluidity, stable concrete while also acting as a viscosity modifier. The retarder used met ASTM C-494 standards [41]. Third-generation chemical admixtures based on poly-carboxylate ether were used as superplasticizers. SP1 is based on Naphthalene Formal-dehyde Sulphonate (Sikament-nn), SP2 is based on modified polycarboxylate ether from Chryso (272), SP3 is based on modified polycarboxylate ether from Chryso (292) and PS is an accelerator plasticizing agent (Xel). The ACI recommends an absolute volume [42].

Experimental work
Concrete mix proportion
The absolute volume method was used to determine the quantities of materials required for the test batch. The mix proportion for each mix is shown in Table 2. Three standard cubes of $150 \times 150 \times 150$ mm and three cylinders of 150×300 mm in dimensions were cast from each batch. The cubes were used to obtain the compressive strength of concrete (f_{cu}), and the cylinders were used to obtain the splitting tensile strength (f_{ctr}).

Casting and testing
Cubes of steel based with size 150 mm $\times$ 150 mm $\times$ 150 mm and cylinders of steel based with size 150 mm $\times$ 300 mm were taken for preparation of concrete mix sample. Concrete materials used in the mix proportion are presented in Fig. 2. Firstly, find out the suitable water-cement ratio by adding a superplasticizer by workability test. After that deciding the suitable admixture proportion from trail mix for preparing different types of concrete mixes. The materials required like cement, water, superplasticizer, fine aggregate, and coarse aggregates were mixed together as per trial mix proportion. After demolding from molds samples of concrete mixes were kept at room temperature and cured for 3 days. The sample was kept to analysis of compressive strength through the compressive machine and split tensile.

Curing of concrete samples
The specimens used to specify the properties of rapid hardening concrete were twenty separate pours. The RHC samples were curried for up to 3 days at laboratory temperature. While the normal concrete samples were cured for up to 28 days at laboratory temperature. Referred to standard conditions given in testing standards such as EN 12390–2:2009 [43].

Mechanical properties
Rheological properties
The rheological properties play a defining role in assessing the performance of fresh concrete mixes based on standard test results. Various tests, including the slump test for normal and rapid hardening concrete, as well as slump flow, L-shape, and V-funnel tests for self-compacting concrete, were conducted. Slump values were measured immediately after mixing and at 10 min, 30 min, and 60 min thereafter, with results detailed in Table 4. The slump flow test, is depicted in Fig. 3. The recommended dosage of poly-carboxylate ether and activator, at 2% and 0.47%, respectively, was determined by the weight of cementitious materials with a water-to-cement ratio of 0.25. This dosage was established under ambient conditions of 22 °C and 26% humidity. Table 4 and Figs. 3

Table 2 Mix proportions of the concrete mixes (kg/m³)

Mix	designation	Cement kg/m³	Microsilica (kg)	C.Agg kg/m³	F. Agg kg/m³	Water L	Super plasticizers Plasticizing agent (L)				Retarder (L)	w/c	Type of mix
							SP1	SP2	SP3	PS			
M1	A	475	–	1200	500	190	10	–	–	–	–	0.40	RHC
M2	A	475	25	875	884	174	–	–	12.5	2	–	0.35	RHC
M3	B	500	25	960	777	165	–	–	14	–	–	0.31	RHC
M4	A	475	–	1200	500	190	12.5	–	–	–	3	0.40	RHC
M5	A	475	25	875	884	174	–	–	12.5	–	–	0.35	SCC
M6	A	475	25	875	884	174	–	10	–	3	–	0.35	SCC
M7	B	500	25	960	777	165	–	–	14	–	–	0.31	RHC
M8	B	500	25	960	777	165	–	–	10	1	–	0.31	RHC
M9	C	500	25	960	777	165	–	–	10	1	–	0.31	RHC
M10	B	475	25	875	884	174	–	10	–	3	–	0.35	RHC
M11	B	600	35	912	737	158	–	–	13	3	–	0.25	RHC
M12	B	650	50	846	683	175	–	–	14	4	–	0.25	RHC
M13	B	550	31	836	675	165	–	–	11	3	–	0.28	RHC
M14	B	600	42	895	730	180	–	–	14	4	–	0.28	RHC
M15	B	700	60	1024	860	225	–	–	17	5	–	0.30	RHC
M16	B	575	35	874	706	180	–	–	14	4	–	0.30	RHC
M17	B	600	35	895	737	158	–	–	13	3	–	0.25	RHC
M18	B	600	35	895	737	300	–	–	–	–	–	0.47	NC
M19	C	500	–	987	798	320	–	–	–	–	–	0.64	NC
M20	B	500	25	960	777	250	–	–	–	–	–	0.48	NC

Mix A Cem I 42.5N, Mix B Cem I 52.5N, Mix C Cem III 42.5N, SP1 super plasticizer (Sikament-nn), SP2 superplasticizer (Chryso 272), SP3 super plasticizer (Chryso 292), PS accelerator plasticizing agent (Xel 666)
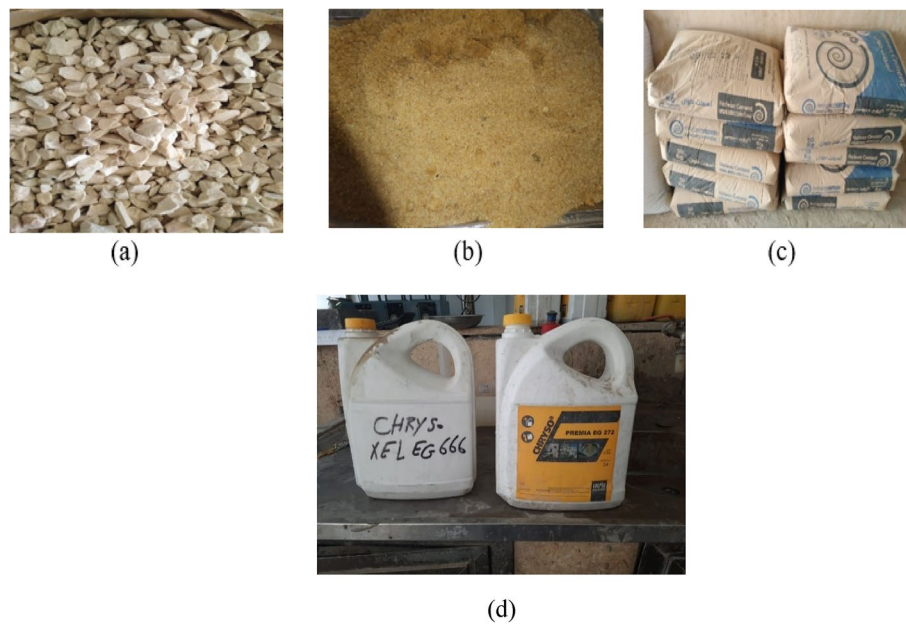
Elfakhrany *et al. Journal of Engineering and Applied Science*   (2024) 71:74

Page 7 of 20

(a)   (b)   (c)

(d)

Fig. 2 Concrete materials: **a** coarse aggregate, **b** fine aggregate, **c** cement, **d** superplasticizer and plasticizing agent

Fig. 3 Slump test

and 4 demonstrate the influence of ambient temperature on the rheological characteristics of the concrete. Despite temperature changes from 39 °C to 24°C, the presence of polycarboxylate ether ensures minimal impact on slump values, enhancing workability. As the temperature decreases from 40 to 24 °C, and concrete type transitions from SCC to RHC, the behavior of SCC is favored over RHC. Notably, the workability of rapid-hardening concrete mixes surpasses that of normal strength and self-compacting concrete due to the efficiency of admixtures in achieving early strength and improving workability.

Compressive strength test

The compressive strength analysis of the examined concrete samples followed the testing protocol outlined in EN 12390–2:2009 [43]. Utilizing an automatic hydraulic press,

Elfakhrany *et al. Journal of Engineering and Applied Science*   (2024) 71:74

Page 8 of 20

Fig. 4 Test setup for compression test

Fig. 5 Mode of failure of cubes

depicted in Fig. 4, the compression test applied load perpendicular to the specimen. Figure 5 illustrates a compressive test of the specimen and the mode of failure. The results of compressive strength at intervals of 8, 16, 24 h, and 7 and 28 days are detailed in Table 3, showcasing that some mixes can achieve 31 MPa within 8 h. Notably, the use of polycarboxylate ether-based superplasticizers in hot weather yielded strengths 59% higher than in cold weather, as indicated by the results. Various parameters, as illustrated in Fig. 6, have the potential to influence compressive strength outcomes.

The compressive strength can be estimated from the following equation:

$$f_{cu} = P/A \tag{1}$$

where.

f_{cu} = Compressive strength,

P = Compression load at failure, and.

A = Area of cube (150×150 mm).

Splitting tensile strength test

An examination of the tensile strength across different types of concrete was conducted, employing splitting tests in accordance with the specifications outlined in EN 12390–2:2009 [43]. The testing procedures involved an automatic hydraulic press, as depicted in Fig. 7, while the mode of failures of the cylinders is illustrated in Fig. 8. The varied tensile strength values at different ages for the mixes are detailed in Table 3.

It was observed that the utilization of polycarboxylate ether-based superplasticizers enhances the tensile strength of rapid-hardening concrete compared to normal concrete.

Table 3 Compressive and tensile strength of mixes

Trial	weight (gms)	Compressive strength (MPa)						Tensile strength (MPa)				λ
		8H	16H	24H	3D	7D	28D	1D	3D	7D	28D	43.30
1	8228	–	18.7	30.1	55.4	62.9	75	5.3	7.9	8.4	8.5	46.10
2	8306	25	–	45.3	64.2	71.5	85	7.9	9.1	9.5	9.7	48.73
3	8342	27.15	–	50.7	71.6	81.4	95	8.9	10.2	10.5	10.7	38.73
4	8075	–	–	0.6	31.1	47	60	–	4.4	6.3	6.4	43.59
5	8304	27.7	–	43.9	63.4	69.4	76	7.7	9	9.2	9.3	45.06
6	8352	31	–	44.5	60.7	66.9	81.2	7.8	8.6	8.9	8.4	44.44
7	8354	3.6	15.3	24.8	41.4	61.4	79	4.3	5.9	8.2	8.3	44.67
8	8284	5.9	18	24.6	45.1	65.5	79.8	4.3	6.4	8.7	8.9	43.01
9	8348	2.4	14.4	27.4	53.5	59.5	74	4.8	7.6	7.9	8.0	43.56
10	8332	5.3	15.8	24.9	47.7	60.4	75.9	4.4	6.8	8.0	8.2	48.99
11	8334	17.9	29.8	33.2	57.4	88.7	96	5.8	8.2	10.5	10.9	46.10
12	8306	15.7	28.2	30.1	56.2	79.8	85	5.3	8.0	9.6	9.8	45.00
13	8287	15.1	23.4	27.9	49.6	76	81	4.9	7.0	8.4	9.5	43.16
14	8277	12.3	21.9	27.8	51.5	61.5	74.5	4.9	7.3	7.7	8.2	43.87
15	8158	9.6	16.6	27.6	46.3	63.2	77	4.8	6.6	7.9	8.4	45.28
16	8248	10.4	17.7	30.5	45.2	68.4	82	5.3	6.4	8.5	9.0	46.10
17	8200	12.8	21.9	26.9	50.1	60.7	85	4.7	7.1	8.1	8.8	31.86
18	7730	–	–	8.2	14.4	18.8	40.6	2	3.5	4.1	4.9	29.58
19	8368	–	–	4.6	14.5	27.1	35	1.3	3.2	4	4.4	35.36
20	8323	–	–	10	19.9	31.8	50	2.2	3.4	3.8	4.6	43.30

Where λ: modulus of elasticity (GPA)

The influence of various parameters on tensile strength results is depicted in Fig. 9. Tensile strength can be estimated using the following equation:

$$f_{ctr} = 2P/(\pi DL) \tag{2}$$

where.

F_{ctr} = splitting tensile stress,
P = Splitting load at failure,
D = Diameter of cylinder (150 mm), and.
L = Height of cylinder (300 mm).

Modulus of elasticity

The elastic modulus was evaluated at a 40% stress level, and the results are shown in Table 3. The modulus of elasticity also depends on the compressive elasticity of concrete. RHC tends to have a lower modulus of elasticity compared to NC since it has less coarse aggregate. Some studies have shown that NC with the same compressive strength has a higher modulus of elasticity than RHC. As the strength of concrete increases, the difference in elastic modulus between RHC and NC decreases. An increase in compressive strength results increase in the modulus of elasticity. Many other factors, such as the type of aggregate, particle size distribution, type of mix proportion, concrete age, and curing process, also influence this relationship. Concrete containing a larger amount of coarse aggregate has a higher elastic modulus. It was reported that concrete tested in wet conditions has a 15% higher
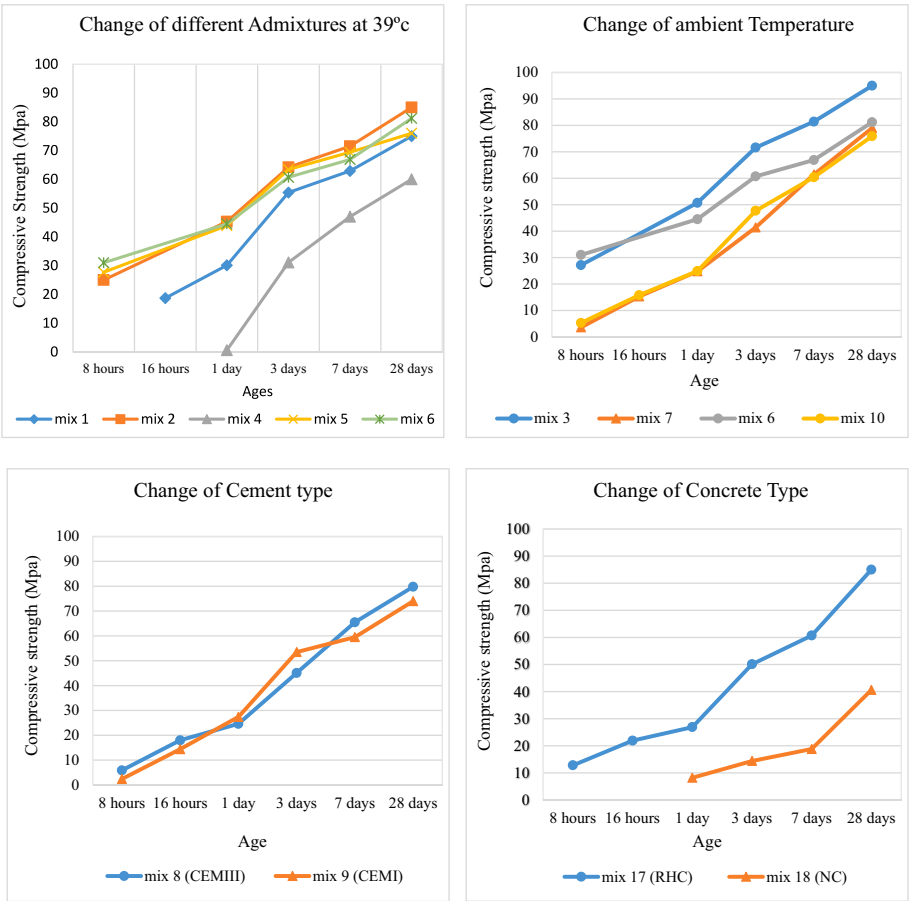
Fig. 6 Effect of compressive strength on different parameters

Fig. 7 Test setup for tensile test
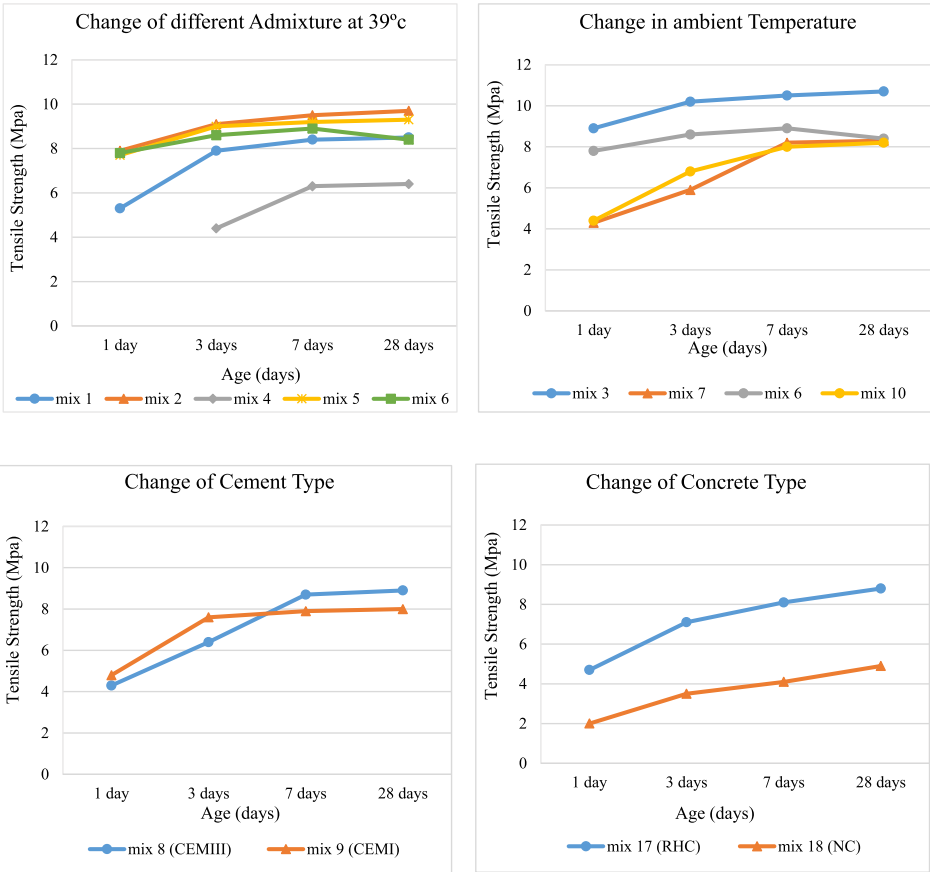

Fig. 8 Modes of failure of cylinders

Fig. 9 Effect of tensile strength on different parameters

Fig. 10 The temperature of the specimen

modulus of elasticity compared to dry conditions. Many researchers have reported that the modulus of elasticity of RHC is lower than that of NC for the same class of strength. Therefore, predicting the modulus of elasticity of RHC is of great significance Fig. 10.

Table 4 The temperature and humidity of the specimen

Trial	Slump (mm)			Temperature	Humidity	Type of concrete
	10 min	30 min	60 min			
1	240	215	200	39 ºC	20%	RHC
2	245	190	170	39 ºC	20%	RHC
3	270	250	220	39 ºC	20%	RHC
4	245	175	160	39 ºC	20%	RHC
5	–	780	760	40 ºC	22%	SCC
6	–	770	750	40 ºC	22%	SCC
7	270	270	250	24 ºC	27%	RHC
8	270	265	260	24 ºC	27%	RHC
9	250	250	240	24 ºC	27%	RHC
10	260	260	250	24 ºC	27%	RHC
11	250	250	240	24 ºC	27%	RHC
12	265	265	260	24 ºC	27%	RHC
13	270	270	260	20 ºC	25%	RHC
14	270	270	270	20 ºC	25%	RHC
15	270	260	260	23 ºC	25%	RHC
16	270	270	270	23 ºC	25%	RHC
17	270	260	250	22 ºC	26%	RHC
18	210	210	190	22 ºC	26%	NC
19	200	200	180	21 ºC	29%	NC
20	95	95	85	21 ºC	29%	NC

Results from the mechanical properties of concrete mixes

The effect of temperature and humidity

The influence of ambient temperature on both strength gain and workability is depicted in Table 4. Temperature readings were taken post-concrete mixing and at intervals using a slump test. Mixes from (1) to (6) were executed during the summer, experiencing an average temperature of 39 ℃ and humidity of 20%. The heightened temperature in summer expedited early strength gains within the initial hours, accelerating the cement paste's hydration process. In contrast, mixes from (7) to (17) were conducted in winter, with an average temperature of 22 ℃ and humidity of 26%, resulting in comparatively slower early strength development. Humidity defined as the quantity of water vapour in the atmospheric air, tends to rise in winter as temperatures lower. The crack growth increases along with the high temperature which is significantly higher in the specimens having accelerating superplasticizers. Another important issue, the specimens' mass losses were determined due to the failure of the high temperature. Finally, it is suggested that the proportion of superplasticizers be higher in cold weather compared to hot weather.

The effect of polycarboxylate ether-based superplasticizer

This paper explores the impact of varying Polycarboxylate ether dosage on the mechanical properties of rapid-hardening concrete. In Mixes 11, 12, and 17, with a water-to-cement ratio (W/C) of 0.25 and Polycarboxylate ether (PCA) constituting 2% of the

cement content, the average compressive strength is 54.6 MPa, and the tensile strength is 7.8 MPa at 3 days. For Mixes 13 and 14, featuring a W/C of 0.28 and PCA at 2.6% of the cement content, the average compressive strength is 50 MPa, with a tensile strength of 7.1 MPa at 3 days. In Mixes 15 and 16, with a W/C of 0.3 and PCA at 3% of the cement content, the average compressive strength is 45 MPa, and the tensile strength is 6.5 MPa at 3 days. The trend observed is that as W/C and PCA dosage increase, the mechanical properties of rapid-hardening concrete decrease.

Details of the test specimens

To conduct this experimental program, wooden moulds with internal dimensions of 200 mm × 300 mm × 1700 mm were utilized for casting five concrete beams reinforced with high-grade steel bars. The concrete beams were designed from each mix illustrated in Table 5. Mixes (1) and (2) are rapid-hardening concrete mixes that are used to construct two beams. while mix (3) are normal strength concrete mixes, used to construct the reference beam. Prior to casting, the wooden forms were treated with oil to facilitate the easy removal of samples. The moulds were sufficiently rigid to prevent significant movement during the concrete placement process. Before casting the specimens, electrical resistance strain gauges with a resistance of 120 Ω and a length of 6 mm were installed to measure strain in the middle of the two longitudinal tension bars. These strain gauges were fixed to the steel bars using special glue and then covered with water-proofing material for protection. The specimens were cast in the moulds immediately after mixing the concrete, followed by compaction using a vibrator. Subsequently, the specimens were covered with polyethylene sheets to avoid loss of moisture by evaporation, and cured by water for an average of 3 days for RHC beams and 28 days for NC beams. All mixes are cured at 24 ℃ with 29% humidity.

Reinforcement details

The details of the reinforcement for all tested beams are shown in Fig. 11. The main reinforcement was the same in all test specimens as two steel bars with a 12-mm diameter (T12) were used. It was about 0.4% of the cross-sectional area. All beams were under-reinforced to ensure a ductile failure due to the yielding of steel reinforcement. Two steel bars with a 10-mm diameter (T10) are used as top reinforcement for all tested beams.

Test procedure

Specimens were tested for flexure under a four-point symmetric loading test. The spacing between two-point loadings was 500 mm to ensure the pure bending and zero shear

Table 5 The mix design of the beam specimen

Mix	Cement (kg)	Water (kg)	w/c ratio	Coarse aggregate (kg)	Fine aggregate (kg)	micro silica (kg)	SP (L)	PS (L)
Mix 1	500	165	0.31	960	777	25	14	0
Mix 2	500	165	0.31	960	777	25	10	1
Mix 3	500	250	0.48	960	777	25	–	–

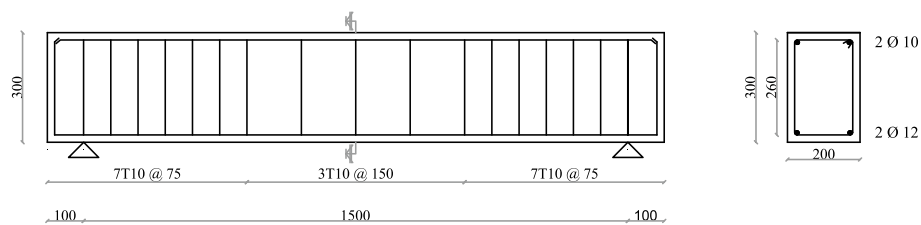*SP* super plasticizer (Chryso 292), *PS* accelerator plasticizing agent (Xel 666)

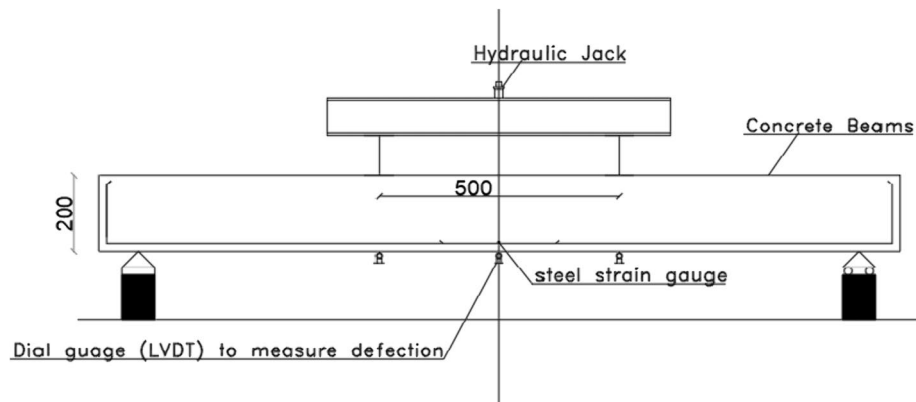**Fig. 11** The details of the test specimens

Fig. 12 The schematic view of the test setup (dimension in mm)

region as shown in Fig. 12. A digital load cell was used in the testing procedure. The capacity of the load cell was 500 KN with an accuracy of 10 KN and was installed at the mid-span of the beam. A hydraulic jack was employed to apply static loads with an increment of 5 KN until failure. During each increment, the load was maintained constant for approximately 10 min while readings were recorded. At each load stage, cracks were marked, and the deflection at the middle and one-third of the span of the beams was measured under the applied loads using three dial gauges with 0.01 mm accuracy. Additionally, the strain at the middle of the tension bars was recorded. Four rapid hardening concrete (RHC) beams and one normal strength concrete (NC) beam as the reference beam were tested in total. All beams had 1700 mm overall length with 1500 mm effective span, 300 mm depth, 200 mm width, and 20 mm as the concrete cover.

Results and discussion

Cracks distribution and failure of specimen

Figure 13 illustrates the crack patterns observed in all tested beams during the failure stage, showcasing the cracking behavior of reinforced concrete beams constructed with rapid hardening concrete (RHC) replacement under four-point bending tests. In each case, the beams demonstrated a gradual and ductile flexural failure, initiating the formation of multiple fine vertical cracks at midspan during the early loading stages. As the applied loads increased, the number of cracks propagating from midspan also increased. The flexural cracks initially developed at midspan and subsequently extended to the shear spans at higher loads. Approaching failure, existing cracks widened with branching, eventually leading to concrete crushing. An analysis

Fig. 13 Crack pattern for all tested beams

Table 6 The results of the flexural test of beams

Beam number	Crack stage			Ultimate stage			Failure stage		
	Load (kN)	Def (mm)	Steel strain (× 10^6)	Load (kN)	Def (mm)	Steel strain (× 10^6)	Load (kN)	Def (mm)	Steel strain (× 10^6)
B1	34.50	2.72	250	90.88	19.94	2056	75.53	46.75	4912
B2	31.01	1.41	178	100.10	22.27	3375	78.29	55.93	4312
B3	42.05	2.59	1140	101.73	13.58	3110	23.56	41.65	4913
B4	40.22	4.17	245	94.88	23.42	2100	76.14	58.02	4150
B5	16.82	2.61	411	64.61	34.52	4630	13.99	57.75	6230

of the crack patterns revealed that all tested beams exhibited a ductile flexural failure mode, particularly noticeable in RHC beams compared to normal concrete beams. The presence of superplasticizers in RHC contributed to an increase in crack, ultimate, and failure loads.

Failure load, deflection, and strains

Table 6 summarizes the results of the flexural test of tested beams. The load, deflection, and steel reinforcement strain at the crack stage, ultimate stage, and failure stage were listed.

Load–deflection relationship

The load–deflection curve for both rapid hardening concrete (RHC) and normal concrete beams is depicted in Fig. 14 for reinforced concrete beams. A characteristic load–deflection response was observed, featuring an initial linear behavior that transitions into rapidly increasing curvature, with a slight deflection increase up to the point of failure. Notably, the RHC beams exhibited a yield load increase of approximately 120% compared to the control beam, and the ultimate load capacity increased by an average of 50% in comparison to the control case. Toward the end of the tests, the failure load for the RHC beams showed a significant average increase of 350% when compared to the normal concrete beams.

Load–strain curve

The steel strain at the middle of the deformed bar in the beams is depicted in Fig. 14. The deflection, yield, and failure loads are determined by load-strain curves, as shown in Fig. 15. The strain of steel is primarily determined by its tensile strength. Consequently, concrete beams that were hardened quickly had a higher tensile strength than beams that had normal strength.

Stiffness and ductility and toughness

Table 7 summarizes the comparisons of the initial stiffness, post-yield stiffness, ductility index, and toughness.

Stiffness

Beam stiffness, defined as the load–deflection curve slope, is an important structural property. The pre-yield (K1) and post-yield (K2) stiffness were calculated using Eqs. (3) and (4).

$$(k1) = \frac{Py}{\Delta y} \tag{3}$$

$$(k2) = \frac{Pu - Py}{\Delta u - \Delta y} \tag{4}$$
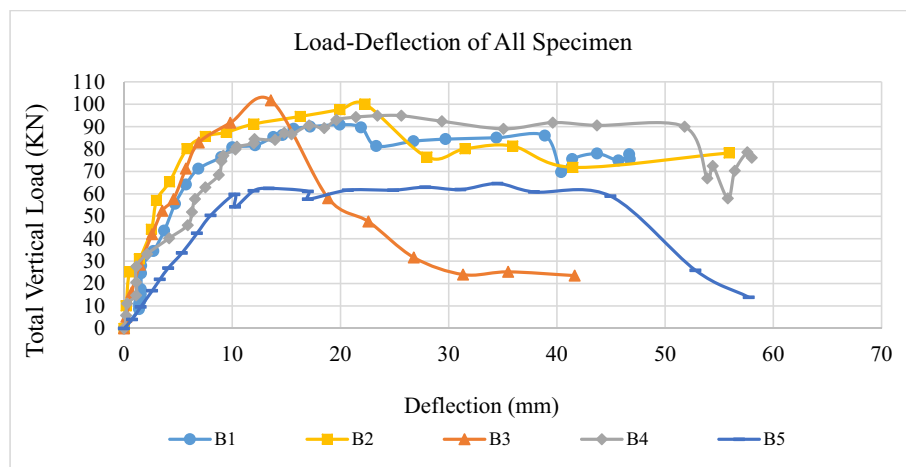
Fig. 14 Load–deflection relationship for the tested beams
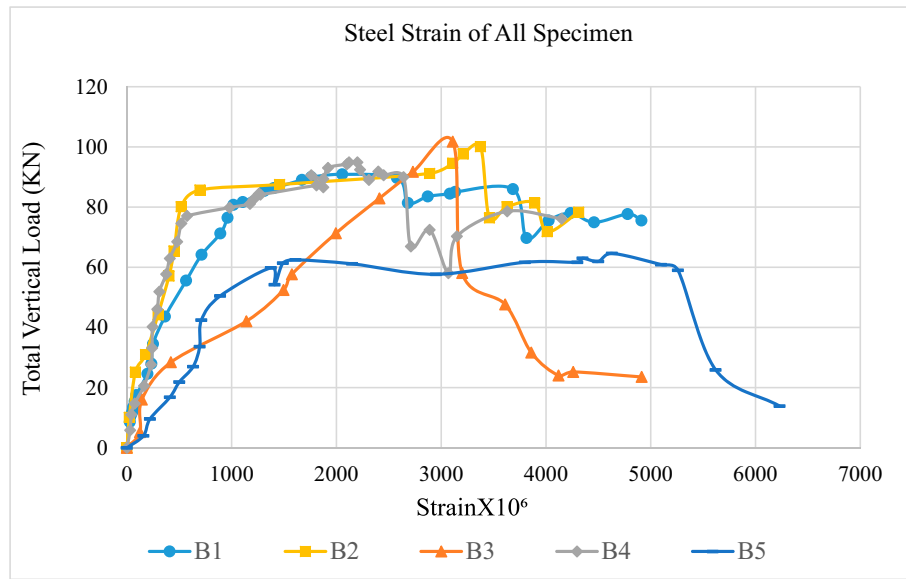
Fig. 15 Load-strain relationship for the tested beams

Table 7 Comparisons of the initial stiffness, yield stiffness, ductility index, and toughness

ID	Yield load P_y (kN)	Ultimate load P_u (kN)	Yield deformation $\triangle y$(mm)	Ultimate deformation $\triangle u$(mm)	Initial stiffness K_1 (kN/mm)	Effective stiffness K_2 (kN/mm)	Ductility µ $\triangle$	Toughness (Joule)
B1	34.5	90.88	2.72	19.936	12.68	3.27	7.33	3200
B2	31.01	100.098	1.40	22.27	22.15	3.31	15.91	4400
B3	42.05	101.727	2.59	13.577	16.24	5.43	5.24	2100
B4	40.22	94.878	4.171	23.416	6.47	1.50	13.28	4200
B5	16.82	64.614	2.60	34.517	9.64	2.84	5.61	2700

where Py is yield load, $\triangle$ y is deflection at yield, Pu is ultimate load, and $\triangle$ u is deflection at ultimate.

The initial and effective stiffness of rapid hardening concrete beams is higher than normal strength concrete.

Ductility

Ductility is a measure of a material's ability to undergo significant plastic deformation prior to rupture or failure [44]. It is quantified as the ratio of maximum displacement to yield displacement (µ), as shown in Eq. (5):

$$\mu = \Delta \mathbf{u}/\Delta \mathbf{y} \qquad (5)$$

where Δ u is the ultimate deformation and Δ y is the yield deformation.

Generally, improved ductility of a structural member indicates an enhanced ability to undergo large deformations before failure, thereby the rapid hardening concrete is more ductile than normal strength concrete.

Toughness

Toughness refers engineering-wise to a material's ability to absorb energy and deform plastically without fracture, proportional to the stress–strain curve area up to failure. It indicates energy absorption before rupture, depends on strength, ductility, and modulus, and enables more energy absorption before failure, which is important for concrete's earthquake and impact resistance. Toughness is typically measured in energy per volume units. It was found that rapid-hardening concrete beams have a higher toughness than normal concrete beams.

Conclusions

[1] The use of proprietary rapid-hardening concrete is necessary when early strength is needed. The use of 2% polycarboxylate ether admixture can result in 50 MPa within 3 days.

[2] The tensile strength of RHC in 3 days is nearly double that of NC, and it is equivalent to 14% of its compressive strength.

[3] The compressive strength of the mixes cast in summer is higher than that of winter mixes by approximately 25% for NC and 92% for RHC mixes. In hot weather, polycarboxylate ether can provide better performance than in cold weather, but it's important to examine how shrinkage cracks affect it.

[4] The flexure properties of rapid-hardening concrete beams show a higher level of ductility, toughness, and deformability when compared to normal-strength concrete. Subsequently, curvature ductility, deflections, crack widths, and energy absorption had a significant increase. The modulus of elasticity of RHC was lower because of the contribution of aggregates.

Recommendation for future study

1-Study the effect of RHC on the flexural performance of different concrete elements.

2-Study the recent type of Admixture that improves the strength and workability of RHC.

Availability of data and materials
All data are available.

Declarations

Ethics approval and consent to participate
No ethics approval is required.

Consent for publication
Applicable because the manuscript doesn't contain individual personal data.

Competing interests
The authors declare that they have no competing interests.

References

1. Singhal S, Chourasia A, Kajale Y, Singh D (2021) Behaviour of precast reinforced concrete structural wall systems subjected to in-plane lateral loading. Eng Struct 241:112474. https://doi.org/10.1016/j.engstruct.2021.112474
2. Mohamed HH, Ibrahim AH, Soliman AA (2021) Toward reducing construction project delivery time under limited resources. Sustainability 13(19):11035. https://doi.org/10.3390/su131911035
3. Su Y, Luo B, Luo Z, Huang H, Li J, Wang D (2022) Effect of accelerators on the workability, strength, and microstructure of ultra-high-performance concrete. Materials 15(1):159. https://doi.org/10.3390/ma15010159
4. Jamei E, Mortimer M, Seyedmahmoudian M, Horan B, Stojcevski A (2017) Investigating the role of virtual reality in planning for sustainable smart cities. Sustainability 9(11):2006
5. Kâzım T (2008) Bond strength of tension lap-splices in full scale self-compacting concrete beams. Turkish J Eng Environ Sci 32(6):377–386
6. Park J-S, Kim YJ, Cho J-R, Jeon S-J (2015) Early-age strength of ultra-high performance concrete in various curing conditions. Materials 8(8):5537–5553. https://doi.org/10.3390/ma8085261
7. Reddy PN, Naqash JA (2020) Review on early strength concrete. EPRA Int J Multidiscip Res Peer Rev J 6(12):116–121. https://doi.org/10.36713/epra2013
8. Zia P, Ahmad SH, Schemmel JJ, Elliott RP (1993) High early strength concrete. Contract 100:205
9. Zemri C, Bouiadjra MB (2020) Comparison between physical–mechanical properties of mortar made with Portland cement (CEMI) and slag cement (CEMIII) subjected to elevated temperature. Case Stud Constr Mater 12:e00339
10. Yasin AK, Bayuaji R, Susanto TE (2017) A review in high early strength concrete and local materials potential, in IOP conference series: materials science and engineering. Inst Phys Publish 267:012004. https://doi.org/10.1088/1757-899X/267/1/012004
11. Janowska-Renkas E (2015) The influence of the chemical structure of polycarboxylic superplasticizers on their effectiveness in cement pastes. Procedia Eng 108:575–583
12. Neville AM (2006) Concrete: Neville's insights and issues. Thomas Telford
13. Perfilov VA, Oreshkin DV, Zemlyanushnov DY (2016) Concrete strength and crack resistance control. Procedia Eng 150:1474–1478
14. Al-musawi H, Huang H, Di Benedetti M, Guadagnini M, Pilakoutas K (2022) Effect of shrinkage on rapid hardening plain and recycled steel fibre concrete overlays. Cem Concr Compos 125:104246. https://doi.org/10.1016/j.cemconcomp.2021.104246
15. Zhao B, Liu C, Wu H, Ge Y, Yang J, Yi Q (2019) Study on out-of-plane flexural stiffness of unstiffened multi-planar CHS X-joints. Eng Struct 188:137–146. https://doi.org/10.1016/j.engstruct.2019.03.023
16. Xiong Z et al (2022) Axial performance of seawater sea-sand concrete columns reinforced with basalt fibre-reinforced polymer bars under concentric compressive load. J Build Eng 47:103828. https://doi.org/10.1016/j.jobe.2021.103828

17. Sun J et al (2021) The effect of graphite and slag on electrical and mechanical properties of electrically conductive cementitious composites. Constr Build Mater 281:122606. https://doi.org/10.1016/j.conbuildmat.2021.122606

18. Zhao BD, Chen Y, Liu CQ, Wu HD, Wang T, Wei XD (2019) An axial semi-rigid connection model for cross-type transverse branch plate-to-CHS joints. Eng Struct 181:413–426. https://doi.org/10.1016/j.engstruct.2018.12.042

19. Feng W, Tang Y, He W, Wei W, Yang Y (2022) Mode I dynamic fracture toughness of rubberised concrete using a drop hammer device and split Hopkinson pressure bar". J Build Eng 48:103995. https://doi.org/10.1016/j.jobe.2022.103995

20. Cao X-Y, Feng D-C, Beer M (2023) Consistent seismic hazard and fragility analysis considering combined capacity-demand uncertainties via probability density evolution method. Struct Saf 103:102330. https://doi.org/10.1016/j.strusafe.2023.102330

21. Fang S et al (2023) Novel FRP interlocking multi-spiral reinforced-seawater sea-sand concrete square columns with longitudinal hybrid FRP–steel bars: Monotonic and cyclic axial compressive behaviours. Compos Struct 305:116487. https://doi.org/10.1016/j.compstruct.2022.116487

22. Bida Z, Ke K, Chengqing L, Li H (2020) Computational model for the flexural capacity and stiffness of eccentric RHS X-connections under brace out-of-plane bending moment. J Struct Eng 146(3):4019227. https://doi.org/10.1061/(ASCE)ST.1943-541X.0002507

23. Cao X-Y, Feng D-C, Wang C-L, Shen D, Wu G (2023) A stochastic CSM-based displacement-oriented design strategy for the novel precast SRC-UHPC composite braced-frame in the externally attached seismic retrofitting. Compos Struct 321:117308. https://doi.org/10.1016/j.compstruct.2023.117308

24. Ghanei A, Eskandari-Naddaf H, Ozbakkaloglu T, Davoodi A (2020) Electrochemical and statistical analyses of the combined effect of air-entraining admixture and micro-silica on corrosion of reinforced concrete. Constr Build Mater 262:120768

25. Rong Q, Hou X, Ge C (2020) Quantifying curing and composition effects on compressive and tensile strength of 160–250 MPa RPC. Constr Build Mater 241:117987. https://doi.org/10.1016/j.conbuildmat.2019.117987

26. Bilodeau A, Malhotral VM (1995) Properties of high-volume fly ash concrete made with high early-strength ASTM Type III cement. Spec Publ 153:1–24

27. Mo F, Li B, Li M, Fang Z, Fang S, Jiang H (2023) Rapid-hardening and high-strength steel-fiber-reinforced concrete: effects of curing ages and strain rates on compressive performance. Materials (Basel) 16(14):4947. https://doi.org/10.3390/ma16144947

28. Yu R et al (2022) Development of a rapid hardening ultra-high performance concrete (R-UHPC): From macro properties to micro structure. Constr Build Mater 329:127188. https://doi.org/10.1016/j.conbuildmat.2022.127188

29. Jackson PJ, Hewlett PC (1998) Portland cement: classification and manufacture. Lea's Chem Cem Concr 4:25

30. Khosla NP, Malpass GA (1997) Use of Large Stone Asphaltic Concrete Overlays of Flexible Pavements (No. FHWA/NC/96-004)

31. Al-Manaseer AA, Aquino EB, Kumbargi H (1999) Properties of concrete containing ultimax rapid-setting hydraulic cement. Mater J 96(5):529–535

32. Chmiel MT (2000) Rapid Hardening Concrete

33. Molenaar AAA (2001) Administarion, PCC pavement evaluation and rehabilitation, Fed. Highw. Adm. Pavement Management Systems, Washingt. DC

34. H Najm P Balaguru M Asce 2005 Rapid-hardening concrete mixes https://doi.org/10.1061/ASCE0899-1561200517:2198

35. Abdraimov I, Kopzhassarov B, Kolesnikova I, Akhmetov DA, Madiyarova I, Utepov Y (2023) Frost-resistant rapid hardening concretes. Materials (Basel) 16(8):3191. https://doi.org/10.3390/ma16083191

36. Cangiano S, Meda A, Plizzari GA (2009) Rapid hardening concrete for the construction of a small span bridge. Constr Build Mater 23(3):1329–1337. https://doi.org/10.1016/j.conbuildmat.2008.07.030

37. G. Cook, Early life flexural performance and behavior of reinforced BCSA concrete beams, 2018. Available: https://scholarworks.uark.edu/etd

38. Ibrahim W, Karim O (2020) Flexural behaviour of reinforced rapid hardened concrete beams. Int J Eng Adv Technol 9:2281–2286

39. Golaszewski J, Cygan G, Golaszewska M (2019) Development and optimization of high early strength concrete mix design, in IOP conference series: materials science and engineering. Inst Phys Publish 471:112026. https://doi.org/10.1088/1757-899X/471/11/112026

40. ECP Committee-203–2020 (2020) The Egyptian Code for Design and Construction of Concrete Structures, Housing and Building Research Center, Giza, Egypt

41. Ahmad JAWAD, Rehman SU, Zaid OSAMA, Manan ANEEL, Beddu S, Ahmad M (2020) To study the characteristics of concrete by using high range water reducing admixture. IJMPERD 10:14271-14278

42. Stacey SM (2016) Evaluation of ASTM C 494 procedures for polycarboxylate admixtures used in precast concrete elements (Doctoral dissertation)

43. Klausen AE, Kanstad, T, Bjøntegaard Ø (2019) Hardening concrete exposed to realistic curing temperature regimes and restraint conditions: Advanced testing and design methodology. Advances in Materials Science and Engineering 2019:1-15

44. Rakhshanimehr M, Esfahani MR, Kianoush MR, Mohammadzadeh BA, Mousavi SR (2014) Flexural ductility of reinforced concrete beams with lap-spliced bars. Can J Civ Eng 41(7):594–604. https://doi.org/10.1139/cjce-2013-0074

Publisher's Note